

HYDROLOGICAL CHARACTERISTICS  
OF WADI EL-ARISH

Zidan, A.R.\* , Owais, T.\*\* and El-Gamal M.\*

ABSTRACT

The overland flow in Wadi El-Arish represents a case of unsteady flow on a pervious surface. The actual flow is the interaction of various additive and subtracting variables; rainfall due to storm, lateral inflow from tributaries, infiltration into the soil and evaporation from the water surface.

The differential equations which govern the overland flow were expressed by the continuity and momentum equations. These two equations were developed to be adaptable for the overland flow problems.

The rectangular grid characteristic method was used for the numerical solution of these two parabolic partial differential equations of the first order.

Wadi El-Arish was represented by a mathematical model to predict the amount of surface runoff obtained due to a storm, in addition to the amount of water infiltrated through the soil.

The numerical solution of the differential equations was accomplished in using computer operations, at the meantime, computations of successive surface profiles yielded informations on the characteristics of surface runoff and infiltration along the whole valley channel.

INTRODUCTION

The prediction of water discharge and characteristics of overland flow on watersheds have been of interest to engineers for many years. The most important aspect of such a problem is the study of flood characteristics in the area subjected to rain storms. The overland flow phenomenon represents a complex problem in the theoretical analysis especially the varying infiltration rate of the soil.

Many investigations were carried out with different approaches, to study some hydrological variables such as infiltration process and the nature of overland flow.

- 
- \* Irrigation and Hydraulics Dept., Faculty of Engrg.,  
Mansoura University.
- \*\* Dean and Head of Water Engrg. Dept., Fac. of Engrg.,  
Zagazig University.

Although both occur simultaneously in nature, the overland flow and infiltration process were separately studied by these investigations through subtracting the infiltration from the rainfall to determine the overland flow. Also some investigations proposed the assumption that the land surface is impervious. However some other investigations of significant application were performed in the field of surface irrigation considering the assumption of a porous surface with certain conditions, for example constant width and constant discharge at the upstream boundary.

Unlike other studies, the present study followed different approach depending on studying the total interaction of the rainfall, runoff, infiltration and evaporation together as they occur in nature concurrently.

The achieved results hoped to be needed by Ministry of Housing, Reconstruction and Land Reclamation to determine the amount of water lost either through infiltration into the soil or that poured into the Mediterranean Sea. Also An evaluation of the amount of saved water which could be stored for various purposes.

#### DESCRIPTION OF THE MODEL AREA

-----

Wadi El-Arish basin lies in the middle and north eastern part of Sinai Peninsula, bounded by latitude  $31^{\circ} 20'$  and  $29^{\circ}$ , longitude  $34^{\circ} 32'$  and  $33^{\circ} 5'$  Fig.(1). It contains an area of 17314.0 square Kilometer. Elevation varies between zero level at the Mediterranean Sea in the north and over 1400.00 ms. above sea level at the upper portion of the drainage area on El-Agma plateau.

The valley channel extends for 268 Kms long from the intake area lying in "Egma plateau" at the confluence of Wadi El-Qisheita to the Mediterranean Sea. In the middle and south parts of Wadi El-Arish are joined by a great number of tributaries are, Wadi El-Qisheta, Wadi El-Biyadh, Wadi Abu-Aligana, Wadi Abu-Tareifiya, Wadi El-Ruaq, Wadi El-Aqaba in South, Wadi Geraia, Wadi El-Shereif, Wadi El-Gurur and El-Muweilah in the middle. Western tributaries are Wadi Abu-Suweira, Wadi Hideidum and Wadi El-Burki Fig.(2).

Five characteristics for the water shed of each tributary are given in Table (1).

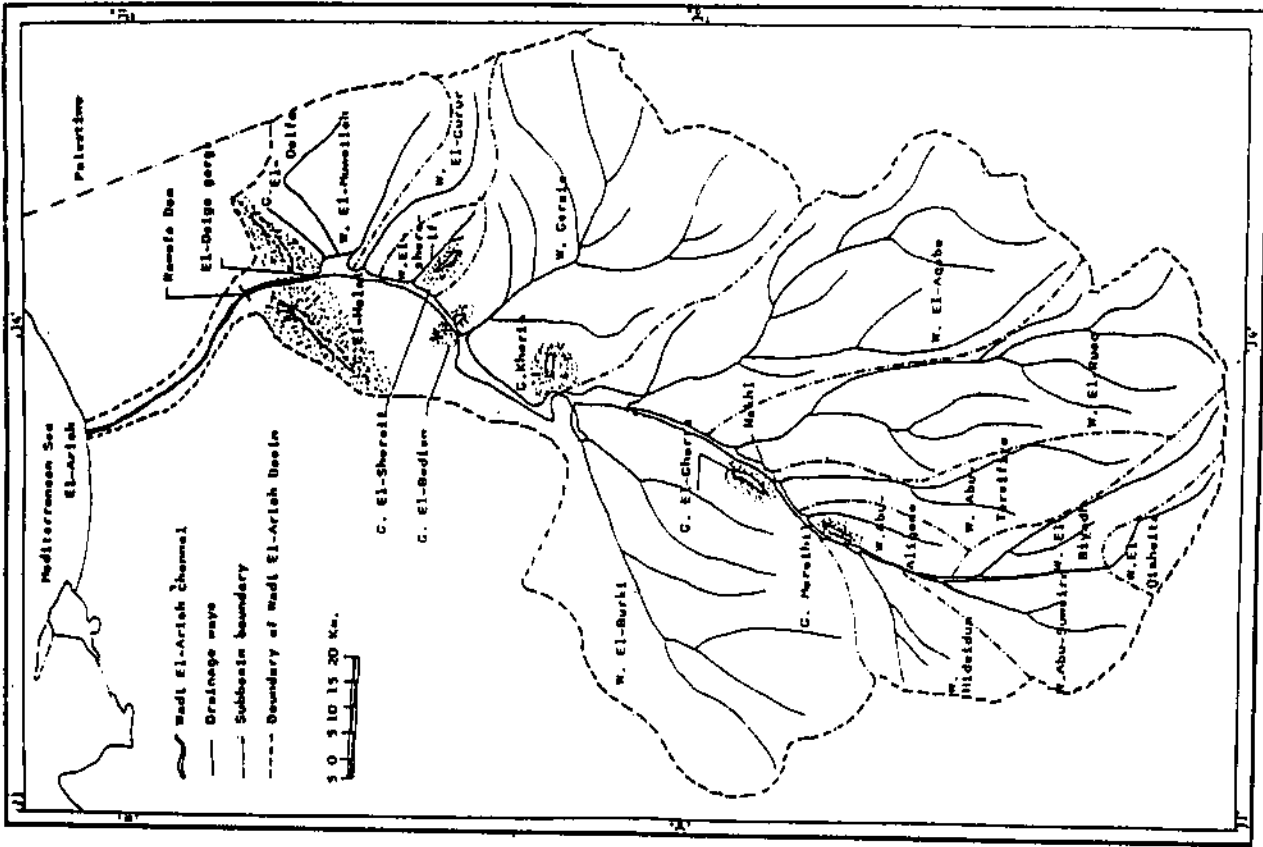


Fig. 2: Pattern of Wadi El-Arish channel and subbasin boundary.

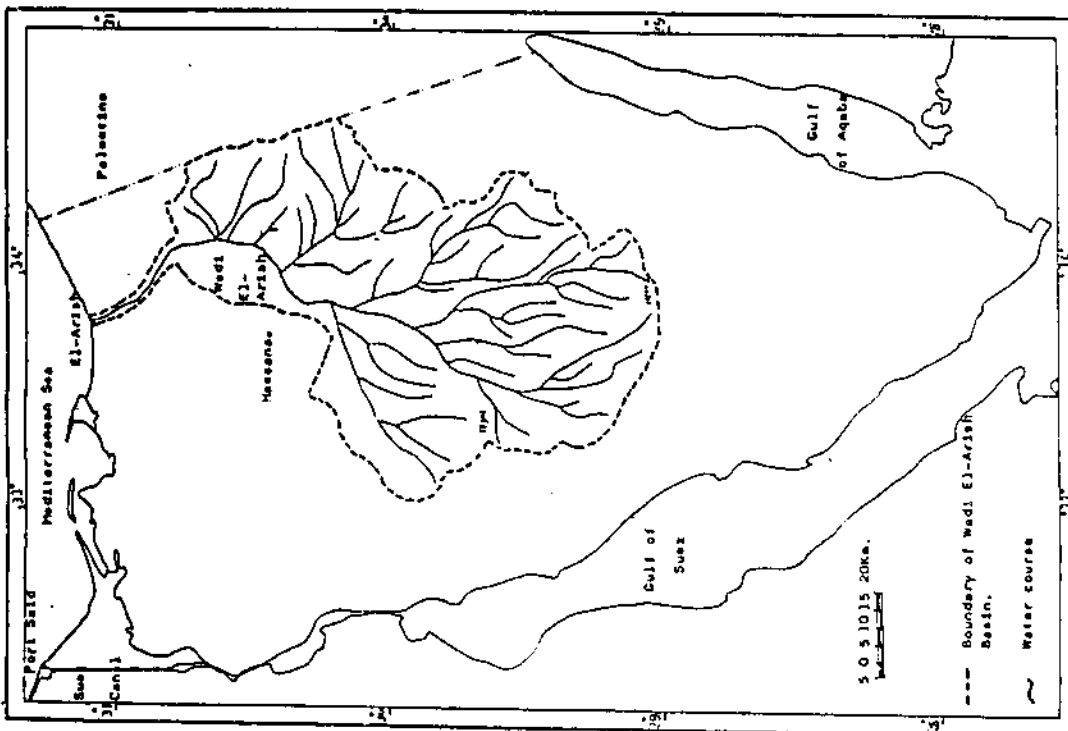


Fig. 1: General outline of Wadi El-Arish basin.

C.4 A.R. Zidan, Owais, and El-Gamal

Table ( 1 ) Characteristics of the watersheds of tributaries in Wadi El-Arish basin.

Name of the tributary	Area Sq.Kms.	Length Km.	Stream density (m per Sq.Km)	Slope	average level
El-Qisheita	330	35	106	0.0085	(1225.00)
El-Biyadh	607	71	116	0.0100	(933.00)
Abu-Suweira	860	42	48	0.0114	(800.00)
Kideidum	800	75	93	0.0150	(720.00)
Abu-Aligana	400	36	90	0.0070	(730.00)
Abu-Tareifiya	955	77	80	0.0045	(740.00)
El-Ruaq	2121	333	157	0.0145	(1000.00)
El-Aqaba	2772	361	130	0.0075	(810.00)
El-Durki	2880	290	100	0.0023	(728.00)
Geraia	2995	310	103	0.0040	(656.00)
El-Shereif	850	60	70	0.0130	(480.00)
El-Gurur	516	52	100	0.0110	(400.00)
El-Muweilah	1040	102	98	0.0044	(570.00)

Table ( 2 ) The values of the roughness coefficient 'n'.

Reach number	Distance, Kms.	$d_{50}$ mm.	$n_0$	n
	0			
1		1.400	0.0554	0.0854
	80			
2		1.520	0.0562	0.0842
	132			
3		0.920	0.0517	0.0916
	184			
4		0.482	0.0465	0.0865
	212			
5		0.900	0.0515	0.0915
	236			
6		1.040	0.0528	0.0828
	244			
7		1.280	0.0547	0.0847
	268			

EXPERIMENTAL PROCEDURE AND FIELD DATA

The numerical values of roughness coefficients, infiltration coefficients and the configuration of cross sections which are necessary for computing the friction effect, the infiltration effect and the change in geometry effect, have to be measured in the field.

Manning's Roughness Coefficients

The roughness coefficients is expressed by the equation Ref.(7)

$$n_o = 0.0525 (d_{50})^{1/6} \quad \dots(1)$$

in which;

$n_o$ : roughness coefficient for straight uniform channel; and

$d_{50}$  = diameter through which fifty percent of the sample in weight can pass.

Seven soil samples, representing the surface soil of each reach were analysed mechanically,  $d_{50}$  for each sample was determined from which  $n_o$  could be obtained Table (2).

Effects of vegetations, channel irregularity, channel alignment, obstructions and meandering of the channel were taken into consideration in evaluating Manning's  $n$  using Cowan formulae Ref.(3). Values of roughness coefficients are given in Table (2).

Infiltration Coefficients

Infiltration equation is expressed as, Ref.(9)

$$i = a.t^b \quad \dots(2)$$

in which;

$i$  = infiltration rate (cm/min.);

$t$  = infiltration time (min.);

$a$  = coefficient which represents the infiltration rate at  $t = 1.0$  (cm/min (1+b))and;

$b$  = dimensionless exponent with values ranging from 0.0 to -1.0.

Wadi El-Arish length was divided into seven reaches according to the soil properties. For each reach the infiltration rate was measured in the field by experimental procedure. Holtan Ref.(8) described several techniques using cylinders infiltrometer, with some modifications in their dimensions, but all have the same basis. In the present study cylinder infiltrometer was used.

The coefficients a and b of equation (2) could be obtained by plotting the experimental data on a double logarithmic paper Figs.(3,4). Values of 'a' and 'b' for different reaches are given in Table (3).

Table (3) Coefficient 'a' and 'b' at different reaches.

Reach number	Distance, Kms.	Coefficient 'a'	Coefficient 'b'
1	0 - 80	3.16	-0.65
2	80 - 132	3.00	-0.70
3	132 - 184	2.08	-0.60
4	184 - 212	2.10	-0.66
5	212 - 236	2.50	-0.57
6	236 - 244	1.90	-0.50
7	244 - 268	1.85	-0.45

#### Section Properties:

The geometrical elements concerning this study are longitudinal slope, and section properties for every increment of 4.0 km length. From the topographic map made by Egyptian Organization Survey, 1936, and drainage map Ref.(12) by ERTS-1 Satellite image 1973. The channel bed levels at certain points were determined and the mean slope for each reach was calculated.

The configuration of cross sections were measured in the field at seven sections along the valley as in Figs.(5,6). The width of the valley channel at some other sections were measured by El-Ramli (5). The widths of the last cross sections were determined from the survey maps drawn to scale 1:100,000.

#### Meteorological Data:

##### (1) Precipitation:

Precipitation falls in the form of scattered heavy rain, occurring in the period from October to May. Precipitation is measured by gauging stations installed on Arish City, Abu-Aweigila El-Quasaima City, Nakl and El-Thamad.

The hydrologic studies were carried out by using the data of Abu-Aweigila, and El-Thamad stations since the data from El-Arish Nakl and El-Quasaima gauging stations were not sufficient due to the lack of duration time.

To determine the average rainfall intensity Thiessen's polygon method, Ref.(11), was used by weighing the rainfall recording gauges according to the area assumed to be represented.

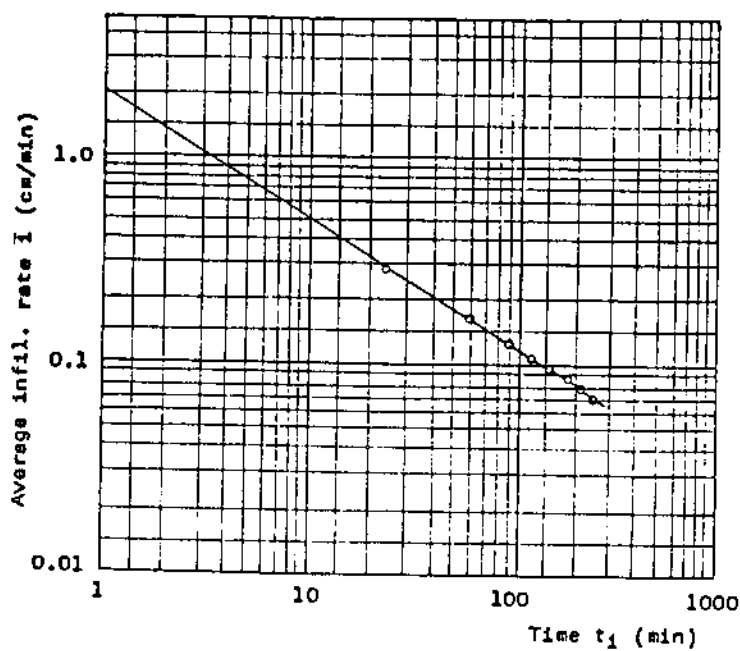


Fig.( 3 ) The measured values of infiltration rates and time on double logarithmic paper at kilometrage 164 along Wadi El-Arish channel.

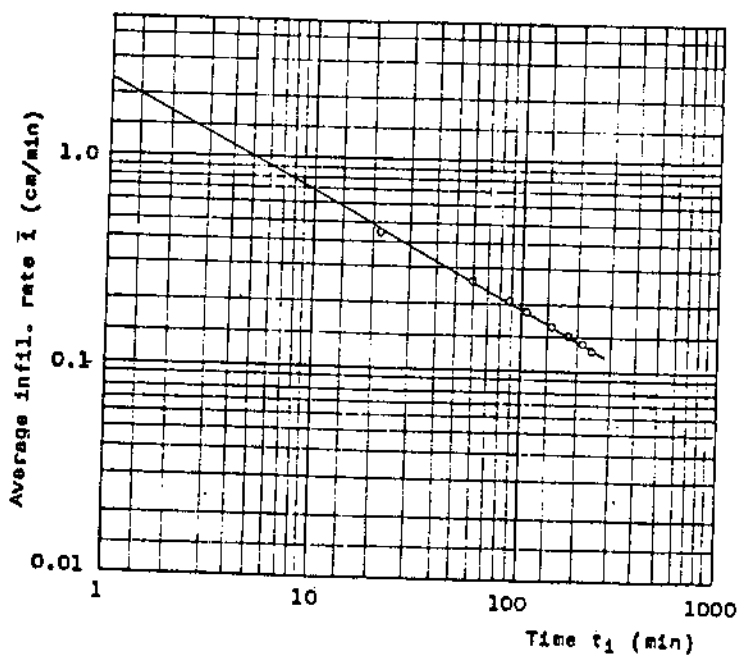
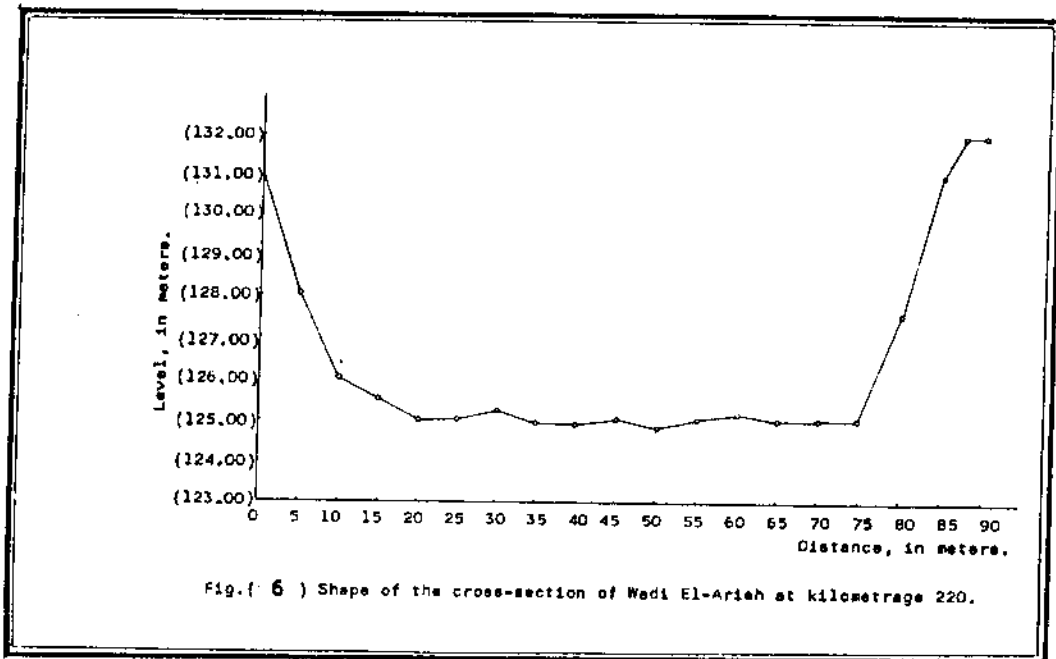
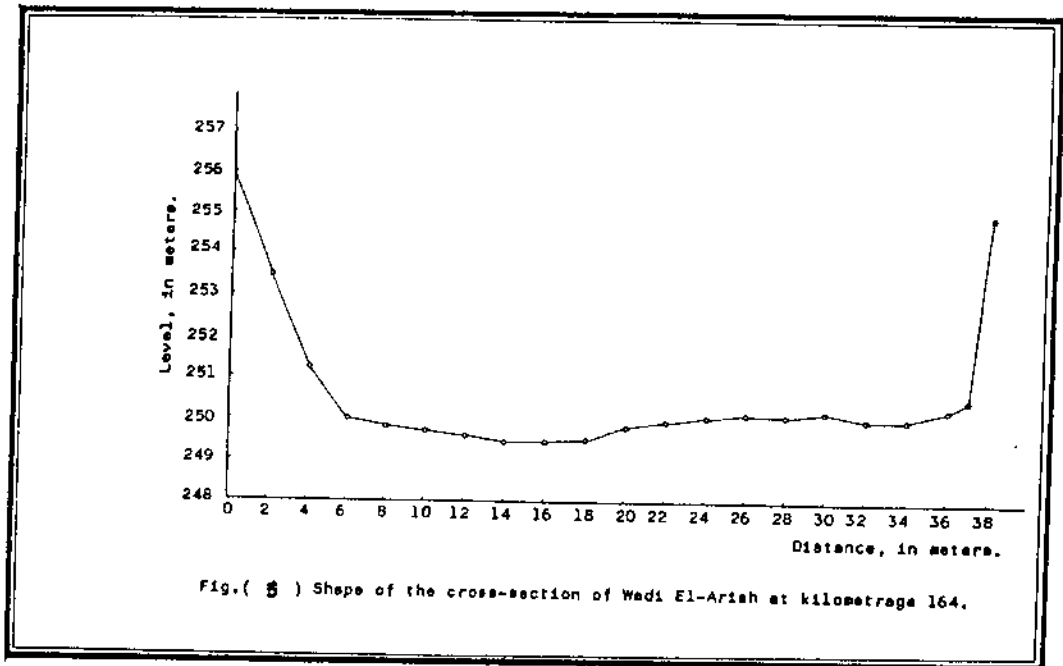


Fig.( 4 ) The measured values of infiltration rates and time on double logarithmic paper at kilometrage 220 along Wadi El-Arish channel.

C.8 A.R. Zidan, Owais and El-Gamal





The average intensity of rainfall during the storm on the basin area (R) = 39.64 mm.

(ii) Evaporation:

The rate of evaporation depending on meteorological data and the nature of evaporating surface. Meteorological data includes, solar radiation, air temperature, humidity, wind speed and atmospheric pressure.

The temperature was found to be more or less constant along the different parts of the wadi. The average rate of evaporation was considered to be constant, neglecting the nil records variation. Applying the equation of Shahtin Ref.(11), the value of evaporation rate (E) was estimated to be  $5.52 \times 10^{-6}$  m/min.

Due to lack in the meteorological data, the source of other hydrological data in the present study was the informations concerning the storm which occurred in Wadi El-Arish on March 18, 1947.

SYNTHETIC HYDROGRAPH

The subbasin area has no runoff measuring stations. Therefore flow hydrographs can not be obtained, instead synthetic hydrographs Fig.(7) have been designed based on known physical characteristics of the subbasin. Synthetic hydrographs were carried out for the aim of determination of peak discharge, time base and lag time. The following equations were used for getting such hydrographs Ref.(10).

Linsely, Kohler and Paulhus's Equation

$$t_p = c_t \frac{(L_1 \cdot L_c) \cdot b_1}{S} \quad \dots\dots(3)$$

in which;

- $t_p$  = lag time in hours;
- $c_t$  = lag time coefficient varies between 0.35 to 1.2;
- $L_1$  = length of the main channel;
- $L_c$  = distance from the outlet to the centroid of the watershed;
- $b_1$  = exponent value equals 0.38, and
- $S$  = basin slope.

C.10 A.R. Zidan, Owais and El-Gamal

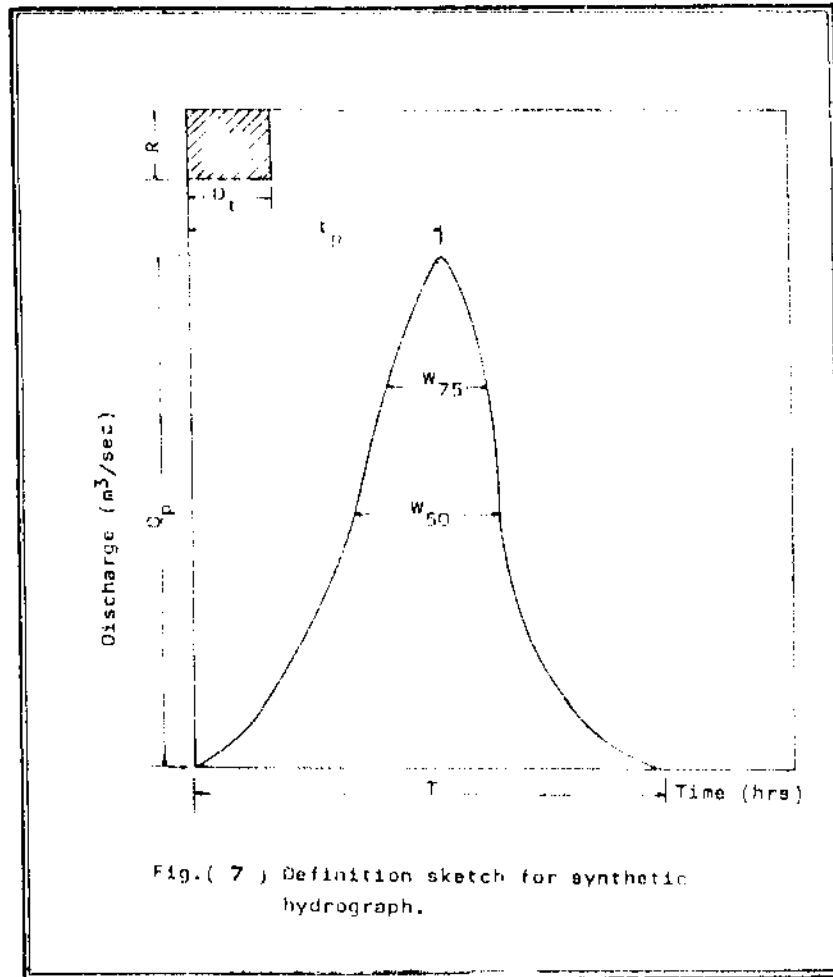


Fig.( 7 ) Definition sketch for synthetic hydrograph.

Table ( 4 ) Synthetic hydrograph parameters for the tributaries in Wadi El-Arish basin.

Name of Wadi	$A_b$ (sq. km.)	$L_1$ (Km.)	$S$	$L_c$ (Km.)	$C_t$	$t_p$ (hr.)	$Q_t$ (hr.)	$R$ (mm.)	$T$ (hr.)	$f$ (%)	$K_1$	$Q_p$ (m <sup>3</sup> /sec)	$q_p$ (m <sup>3</sup> /sec /sq.Km)	$W_{75}$ (hr.)	$W_{50}$ (hr.)
El-Qieheita	330	35	0.0100	15	1.20	31.10			62.2			9.37	0.160	23.26	40.57
El-biyadh	607	71	0.0133	35	1.20	53.24			106.48			10.28	0.093	42.23	73.68
Abu-Suweira	860	42	0.0114	24	1.20	38.64			77.28			19.35	0.129	29.44	51.37
Hideidum	800	30	0.0150	16	1.20	27.87			55.74			25.26	0.179	20.70	36.13
Abu-Aligana	400	36	0.0070	18	1.20	37.13			74.26			9.56	0.134	28.15	49.12
Abu-Tareifiya	955	77	0.0040	45	1.20	55.90			111.80			15.29	0.089	43.97	76.71
El-Ruaq	2121	95	0.0145	50	1.00	55.40			110.80			34.26	0.090	43.37	75.67
El-Aqebe	2772	125	0.0075	75	0.70	55.81	31.2	39.64	111.62	0.46	0.30	44.46	0.089	43.97	76.71
El-Burki	2880	90	0.0045	48	0.82	55.10			110.20			45.12	0.090	43.37	75.67
Gereis	2995	70	0.0040	42	0.85	50.46			100.92			53.03	0.099	39.14	68.29
El-Shereif	850	20	0.0130	8	1.20	20.50			41.00			36.89	0.240	15.00	26.16
El-Gurur	516	52	0.0110	30	1.20	46.00			92.00			10.00	0.108	35.66	62.22
El-Muweilan	1040	40	0.0044	22	1.20	44.24			88.48			20.94	0.113	34.14	59.57

Richard's Equation for peak flow

$$Q_p = 0.1 K_1 \cdot R_m \cdot A_b \quad \dots\dots(4)$$

in which;

$Q_p$  = peak discharge in cumecs;  
 $K_1$  = runoff coefficient;  
 $R_m$  = maximum intensity of rainfall in mm; and  
 $A_b$  = area of the watershed of the tributary.

Sinder's Equation

$$q_p = \frac{c_p}{t_p} \quad \dots\dots(5)$$

$$W_{75} = \frac{3.2}{(q_p)^{1.08}} \quad \dots\dots(6)$$

$$W_{50} = \frac{5.6}{(q_p)^{1.08}} \quad \dots\dots(7)$$

in which;

$q_p$  = maximum discharge per square kilometer;  
 $c_p$  = coefficient ranges from 4.0 to 5.0;  
 $t_p$  = lag time in hours;  
 $W_{75}$  = width of synthetic hydrograph at ordinate 75% of peak discharge; and  
 $W_{50}$  = width of synthetic hydrograph at ordinate 50% of peak discharge.

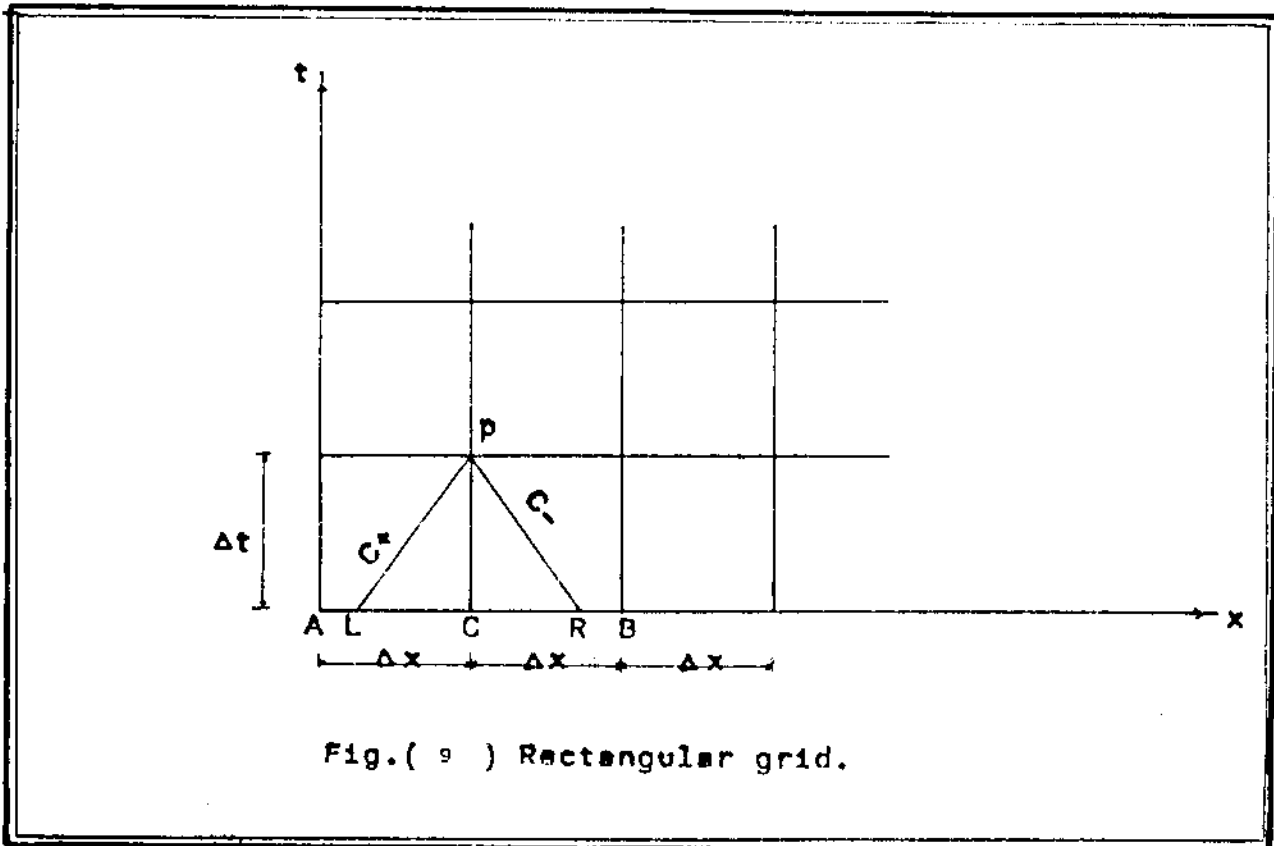
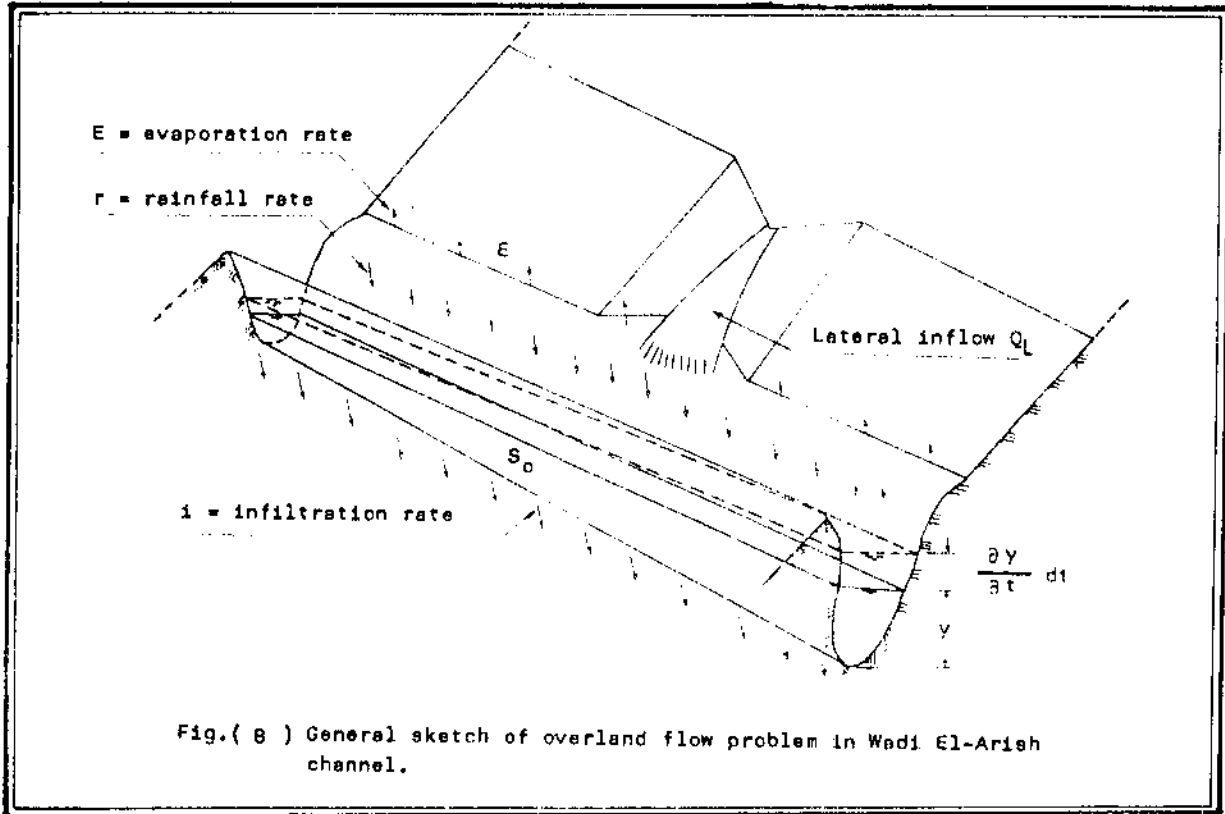
The typical parameters at thirteen tributaries of Wadi El-Arish are given in Table (4).

MATHEMATICAL MODEL

The overland flow in Wadi El-Arish channel is the case of unsteady flow on a pervious surface, resulting from variable inflows, such as rainfall, lateral inflow, infiltration and evaporation rate Fig.(8).

Precipitation rate 'r' falls on the surface of the valley channel which is also feeded laterally with a supplementary discharge  $Q_L$  from the tributaries. Losses from the flow of the channel occur through infiltration rate on the perimeter of the section and evaporation rate from the surface.

C.12 A.R. Zidan, Owais and El-Gamal



Governing Equations

The differential equations of motion governing the overland flow may be established by considering the conservation of mass and momentum in addition to the following assumptions;

- (i) The momentum of precipitation, infiltration and evaporation is so small that it can be neglected;
- (ii) The infiltration rate (i) is evidently non uniform on the perimeter of the cross section. In order to simplify the problem, a uniform infiltration rate is assumed across the top width.
- (iii) The lateral discharge inflow  $Q_l$  from is distributed over the space increment ( $\delta x$ ) Ref.(12).

The general equations of continuity and momentum were derived for overland flow over pervious surface considering rainfall intensity, lateral inflow, infiltration and evaporation Refs.(1,2).

Continuity Equation:

$$\frac{\partial y}{\partial t} + D \frac{\partial u}{\partial x} + u \frac{\partial y}{\partial x} + u \frac{y}{B} \frac{\partial B}{\partial x} = \frac{q}{B} + r - i - E \quad \dots\dots(8)$$

Momentum Equation:

$$\beta \frac{\partial u}{\partial t} + \beta u \frac{\partial u}{\partial x} + g \frac{\partial y}{\partial x} + B \frac{u \cdot q}{BD} + \beta \frac{u \cdot r}{D} - \beta \frac{u}{D} i - \beta \frac{u}{D} E = g (s_0 - s_f) \quad \dots\dots(9)$$

Considering the hydraulic mean depth equals the water depth and the momentum coefficient is unity, the governing equations could be simplified as:

$$\frac{\partial y}{\partial t} + y \frac{\partial u}{\partial x} + u \frac{\partial y}{\partial x} + u \frac{y}{B} \frac{\partial B}{\partial x} = \frac{q}{B} + r - i - E \quad \dots\dots(10)$$

and

$$\frac{\partial u}{\partial t} + u \frac{\partial u}{\partial x} + g \frac{\partial u}{\partial x} = g(s_0 - s_f) - \frac{u}{y} \left( \frac{q}{B} + r - i - E \right) \quad \dots\dots(11)$$

Method of Solution

The method of characteristics was chosen for the numerical solution of equations (10) and (11). The rectangular grid technique has been selected for such solution Ref.(12). The two equations yield the condition, referring to Fig.(9); along the positive (C<sub>+</sub>) characteristic

$$\frac{dx}{dt} = u + (gy)^{1/2} \quad \dots\dots(12)$$

$$\int_L^P du + \int_L^P (g/y)^{1/2} dy - \int_L^P g S_o dt + \int_L^P g S_f dt + \int_L^P \frac{u(gy)^{1/2}}{u+(gy)^{1/2}} \frac{dB}{B} + \int_L^P \frac{q}{By} (u - (gy)^{1/2}) dt + \int_L^P \frac{r}{y} (u - (gy)^{1/2}) dt + \int_L^P \frac{i}{y} (-u + (gy)^{1/2}) dt + \int_L^P \frac{E}{y} (-u + (gy)^{1/2}) dt = 0 \quad \dots\dots(13)$$

along the negative (C<sub>-</sub>) characteristic

$$\frac{dx}{dt} = u - (gy)^{1/2} \quad \dots\dots(14)$$

$$\int_R^P du - \int_R^P (g/y)^{1/2} dy - \int_R^P g S_o dt + \int_R^P g S_f dt - \int_R^P \frac{u(gy)^{1/2}}{u-(gy)^{1/2}} \frac{dB}{B} + \int_R^P \frac{q}{By} (u + (gy)^{1/2}) dt + \int_R^P \frac{r}{y} (u + (gy)^{1/2}) dt + \int_R^P \frac{i}{y} (-u - (gy)^{1/2}) dt + \int_R^P \frac{E}{y} (-u - (gy)^{1/2}) dt = 0 \quad \dots\dots(15)$$

Setting

- B<sub>S</sub> = slope effect =  $g \int s_o dt$
- F<sub>S</sub> = friction effect =  $\int -g s_f dt$
- D<sub>A</sub> = change in geometry effect =  $\int \frac{u(gy)^{1/2}}{u \pm (gy)^{1/2}} \frac{dB}{B}$
- Q<sub>I</sub> = lateral inflow effect =  $\int \frac{q}{By} (-u \pm (gy)^{1/2}) dt$
- R<sub>I</sub> = rainfall effect =  $\frac{r}{y} \int (-u \pm (gy)^{1/2}) dt$
- N<sub>I</sub> = infiltration effect =  $\int \frac{i}{y} (u \mp (gy)^{1/2}) dt$
- E<sub>I</sub> = evaporation effect =  $\int \frac{E}{y} (u \mp (gy)^{1/2}) dt$

Equations (14) and (15) could be rewritten in the following simple form.

$$\begin{aligned} (u + 2(gy)^{\frac{1}{2}})_p &= (u + 2(gy)^{\frac{1}{2}})_L + B_{S_{LP}} + F_{S_{LP}} + D_{A_{LP}} \\ &+ q_{I_{LP}} + R_{I_{LP}} + N_{I_{LP}} + E_{I_{LP}} \dots\dots(16) \end{aligned}$$

$$\begin{aligned} (u - 2(gy)^{\frac{1}{2}})_p &= (u - 2(gy)^{\frac{1}{2}})_R + B_{S_{RP}} + F_{S_{RP}} + D_{A_{RP}} \\ &+ q_{I_{RP}} + R_{I_{RP}} + N_{I_{RP}} + E_{I_{RP}} \dots\dots(17) \end{aligned}$$

#### Model Construction

The mathematical model was constructed along Wadi El-Arish channel to calculate at any instant of time along the whole channel length, water velocity, depth, discharge and infiltration quantity. It extended for 268 Km long from the confluence of Wadi El-Qisheita to the Mediterranean Sea with thirteen tributaries.

The numerical values of rainfall rate, evaporation rate, infiltration coefficients, lateral inflow, bed slopes, section properties and roughness coefficients were introduced as input data in the computer processing. The model should have initial water depth and velocity at each section along the whole valley to start computation. Dry condition was assumed i.e. zero values for both velocity and water depth at every section were considered.

In this model two boundary conditions were used, a discharge hydrograph of Wadi El-Qisheita was used as a boundary condition at upstream. On the other hand, another discharge hydrograph was used as a boundary condition at downstream, its values were hypothetically proposed using the given recorded data which was stored and analysed by the computer.

Space increment  $\delta x = 4$  Km. and time increment  $\delta t = 300$  Sec. were found convenient for carrying out the computations.

Testing of results through verification of Rawafa dam indicated no significant difference between measured and computed results Fig.(10).

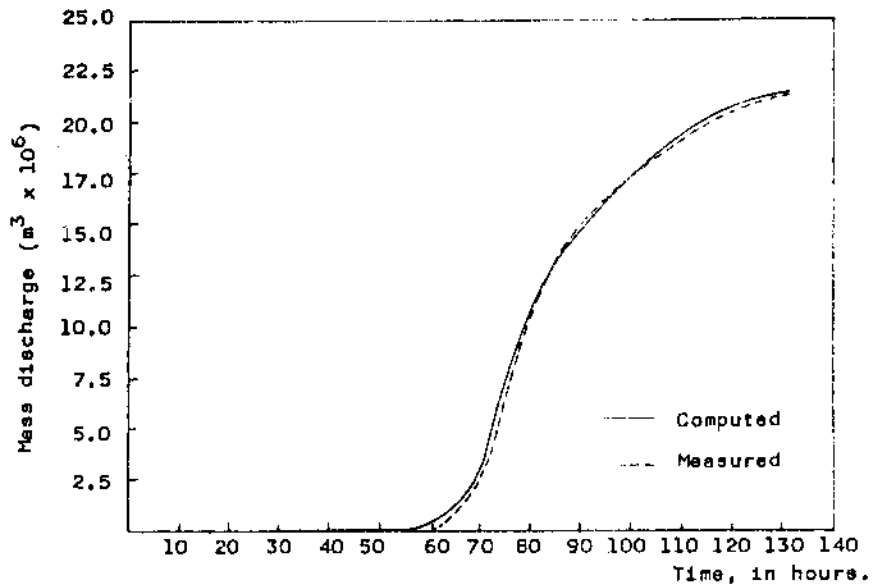


Fig.( 10) Measured compared to computed mass discharge at Rawafa Dam.

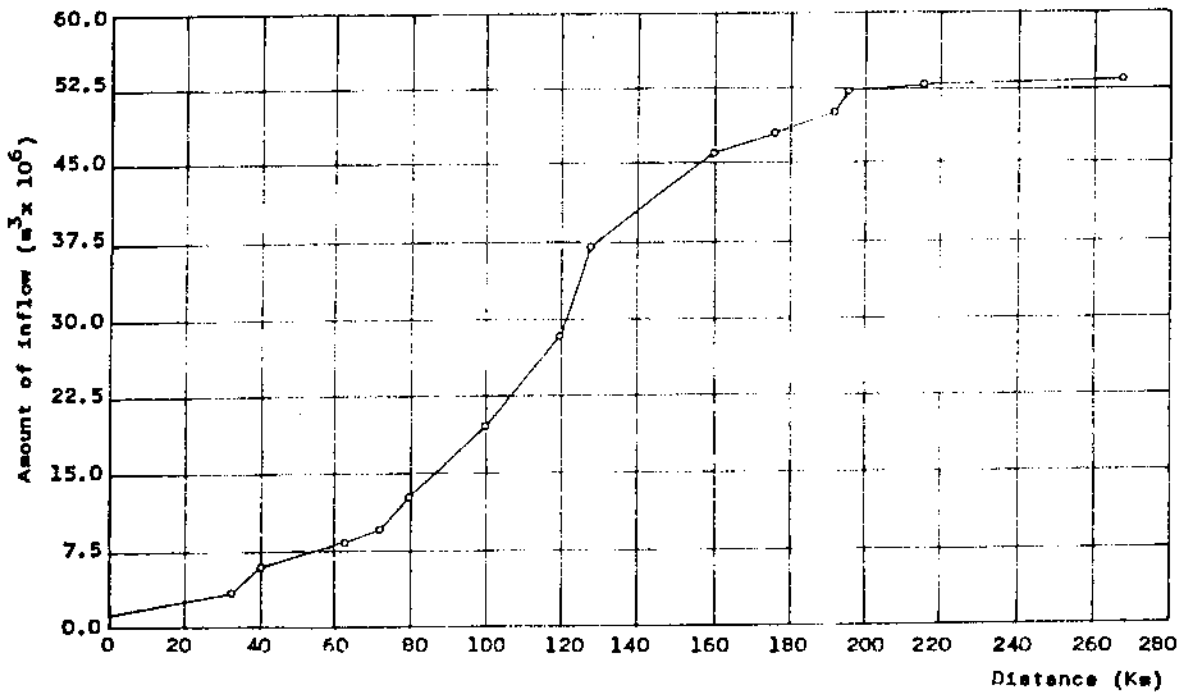


Fig.(11) Sum total amounts of inflow along Wadi El-Arish channel.



### SUMMARY OF RESULTS

-----

Figure (11) shows the total amounts of channel inflow at joining points of the tributaries with the main channel. It indicates that most of the water inflow occurred along a distance from the beginning of the channel to Kilometrage 196, due to the presence of water carrying tributaries along this part of the channel.

The values of maximum depth and that of maximum velocity at any of the 68 sections are shown in Fig. (12) and Fig.(13) respectively. Wide variations between the values of maximum depths at different sections were found ranging from 0.62 m to 3.85 m. Also the values of maximum velocities ranged from 0.5 m/sec. to 1.85 m/sec. These variations were due to differences in the geometrical properties of various sections, and the varied discharge along the valley channel.

The values of peak discharge and corresponding lag time for any of the sixty eight sections along the whole length of the valley are shown in Fig.(14) and Fig.(15) respectively, from which the following points could be concluded:

In the southern and middle parts of the valley, the peak discharge took different values ranging from 6.77 m<sup>3</sup>/Sec. to 242 m<sup>3</sup>/Sec., the minimum value and maximum value occurred at Kilometrage 28 and Kilometrage 196 respectively.

In the northern part the peak discharge decreased gradually as the flow travelled upstream from a maximum of 242 m<sup>3</sup>/sec. at Kilometrage 196 to a minimum value of 138 m<sup>3</sup>/Sec. at Kilometrage 268.

In general the lag time values increased irregularly from south to north. This irregularity in lag time is related to interposition by the tributaries.

The lag time for the part of the channel north to Kilometrage 196 increased regularly towards the north. The regularity of increasing lag time could be explained by the fact that the lag time in this part of the valley was only determined by the channel flow with no interposition by various tributaries having different lag time.

The rate of infiltration at each reach during the flow time is shown in Fig.(16) from which the following points could be observed.

The infiltration rate had the highest value in the last reach near the Mediterranean Sea.

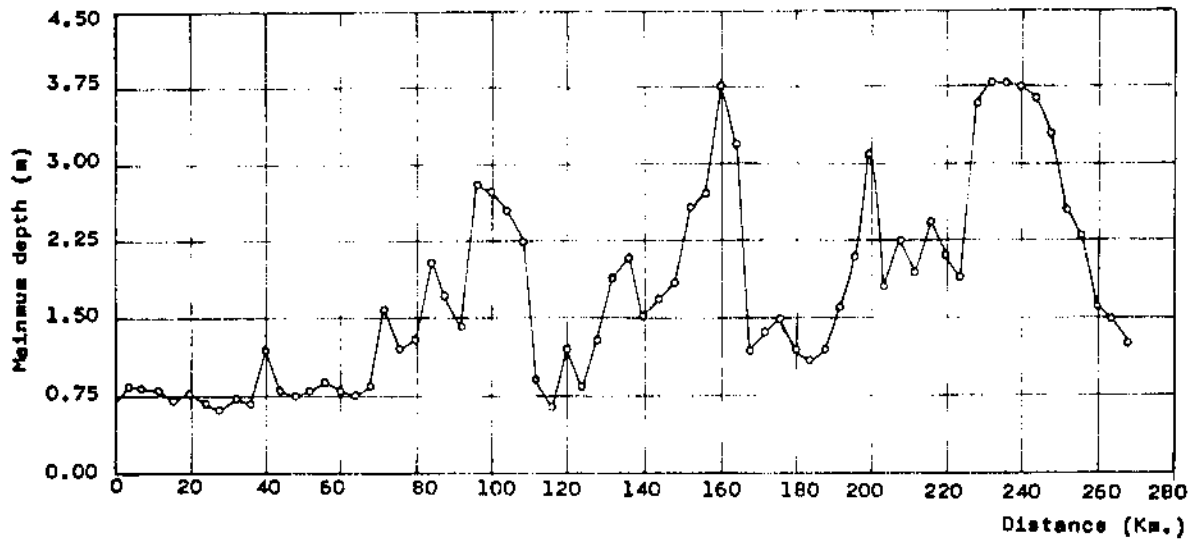


Fig.( 12 ) The values of maximum depth along Wadi El-Arish channel.

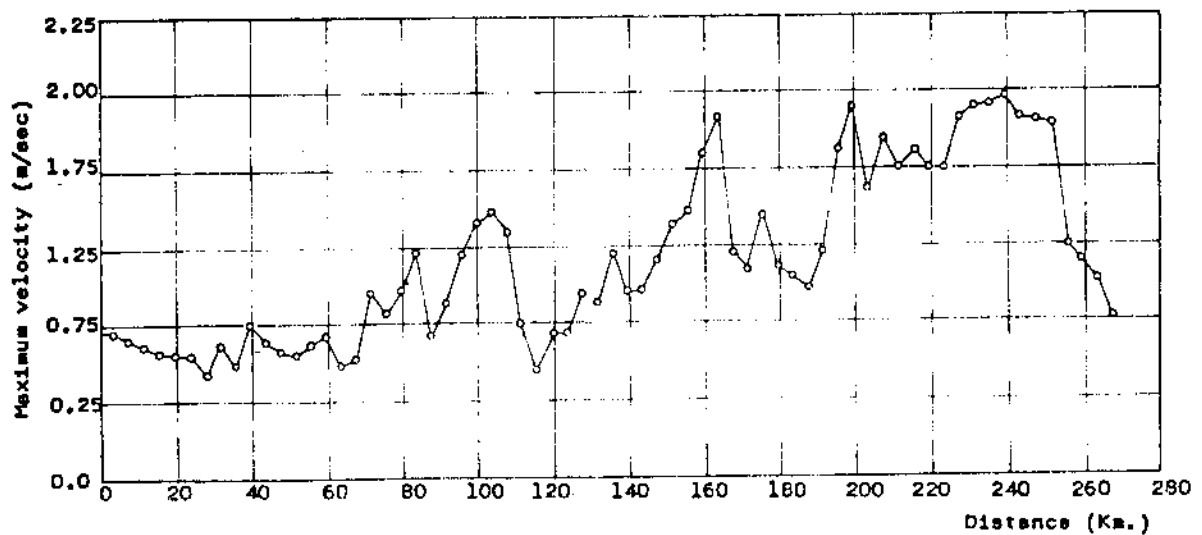
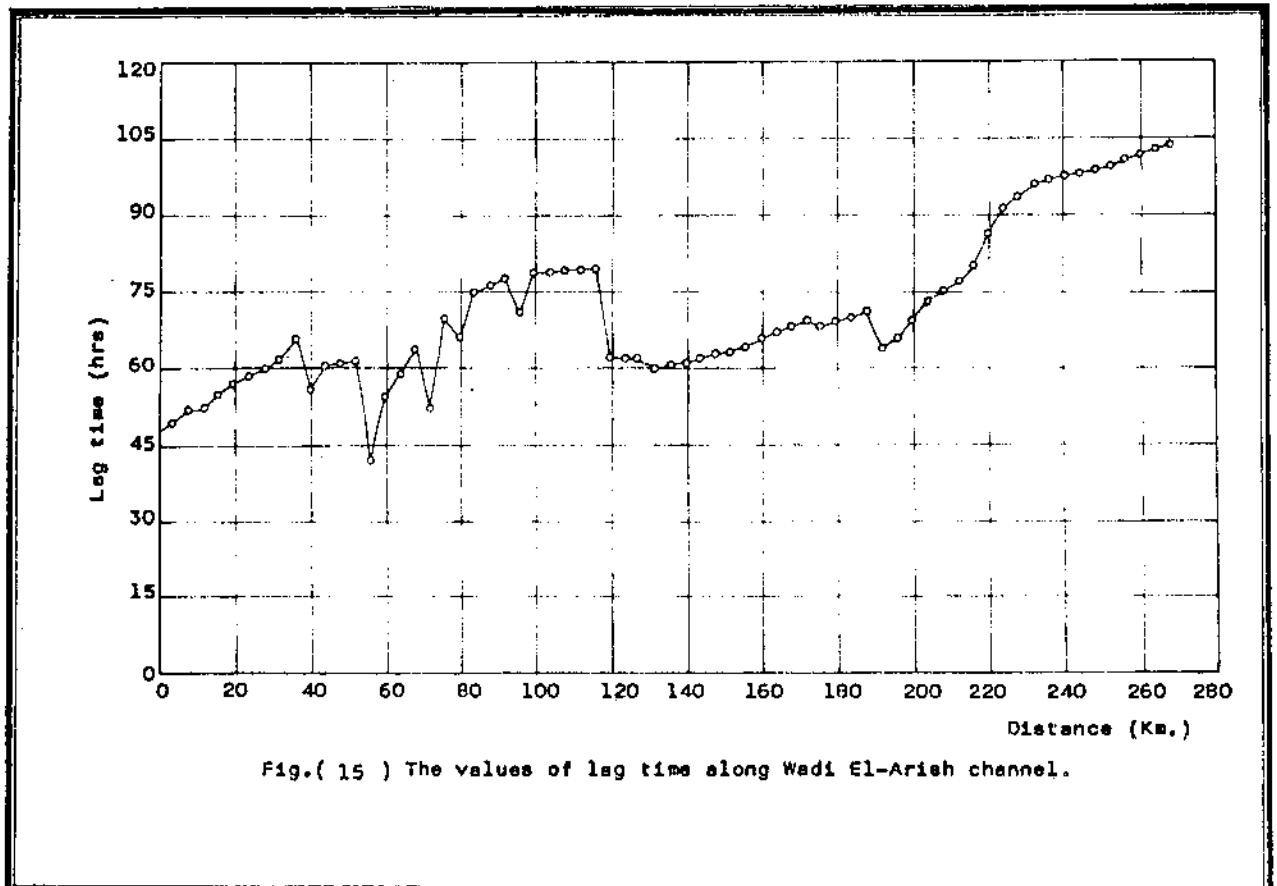
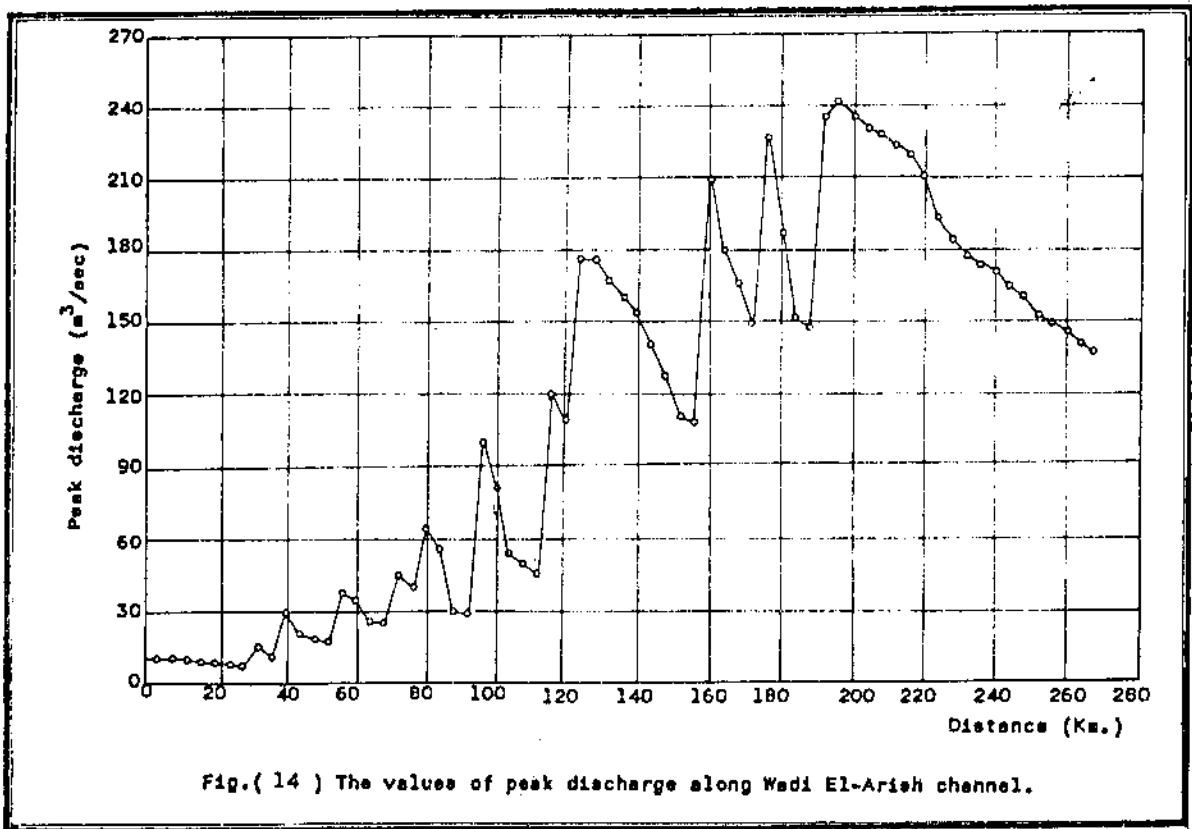
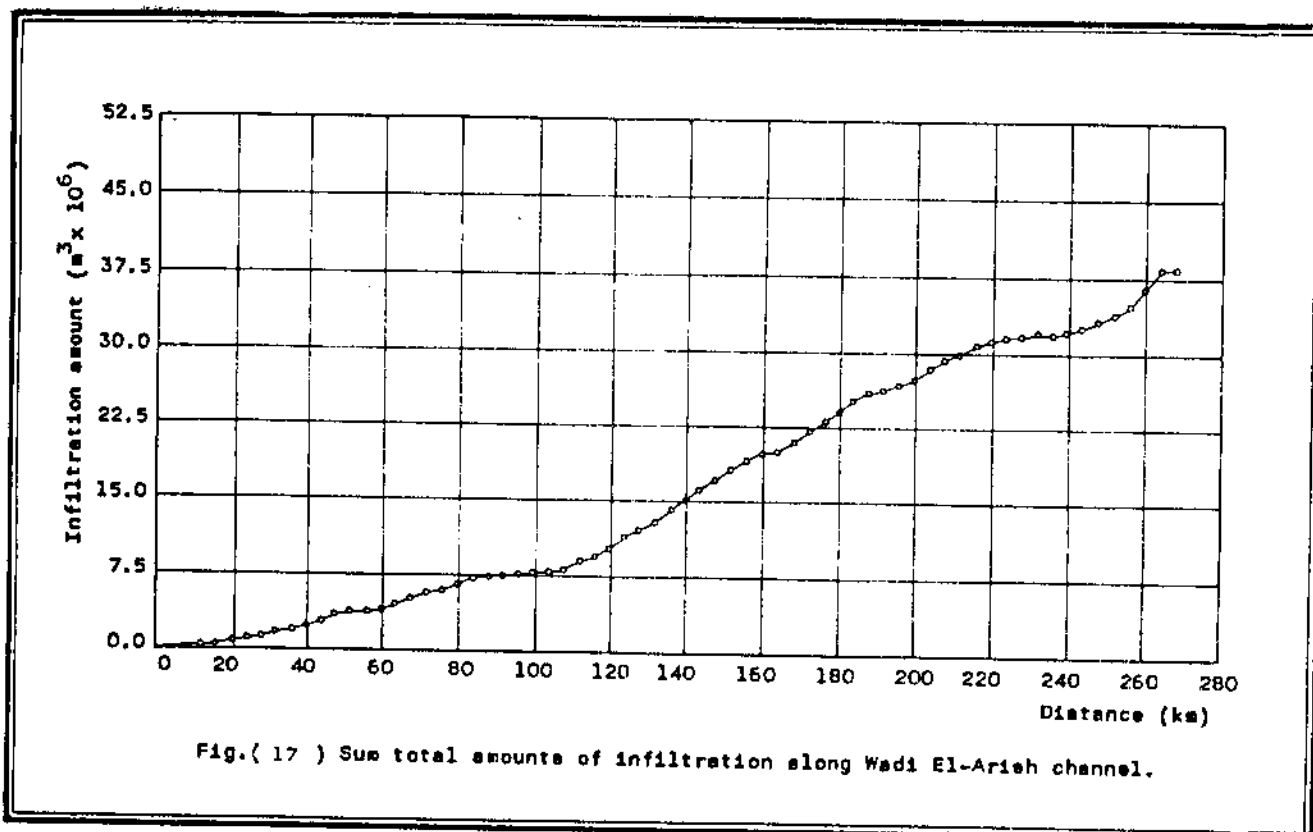
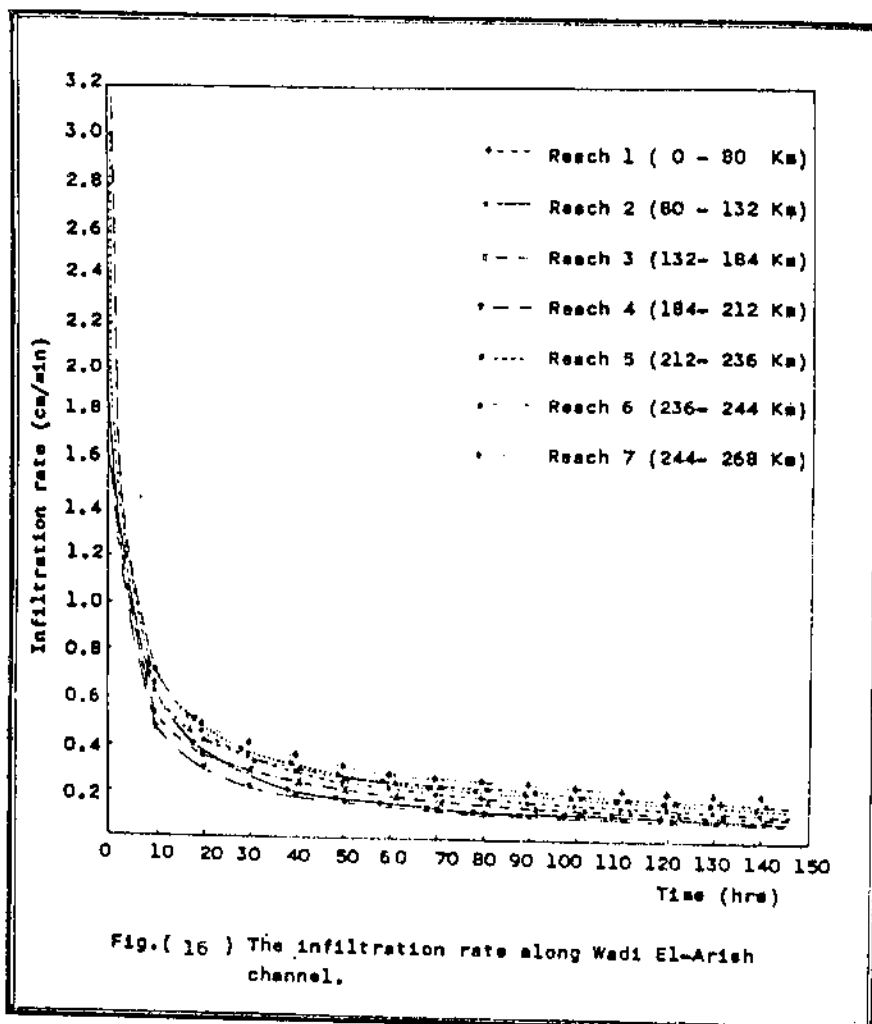


Fig.( 13 ) The values of maximum velocity along Wadi El-Arish channel.



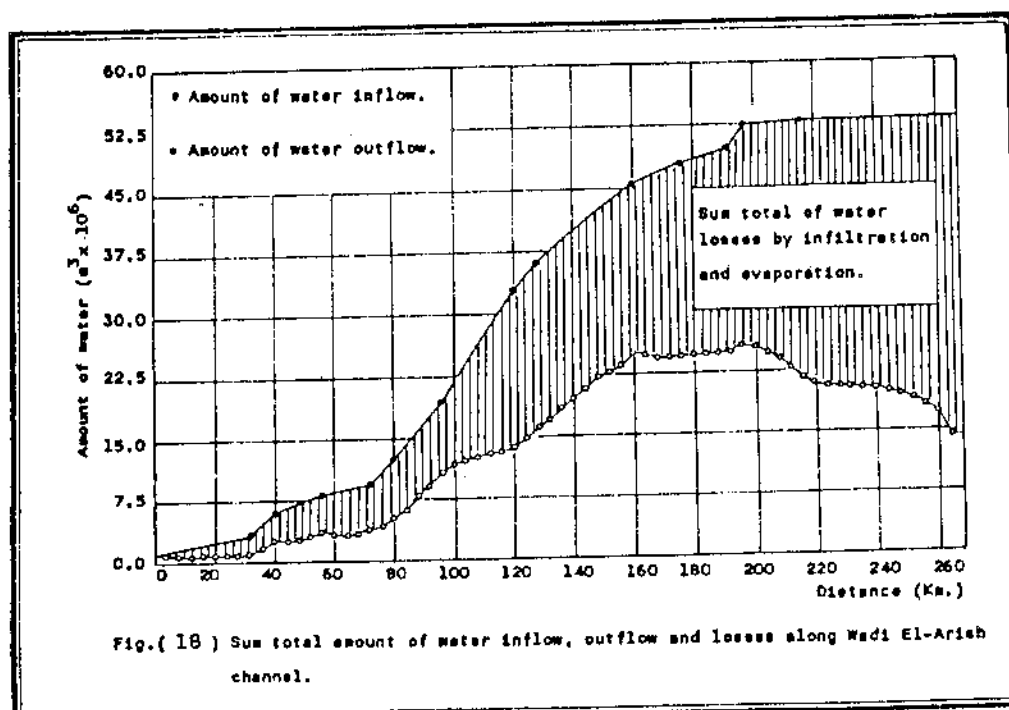


The infiltration rate had the lowest value within a distance bounded between 184 and 212 Kms.

For the other reaches the infiltration rate increased gradually from south to north.

The total amounts of infiltration in Wadi El-Arish channel for each section along its length are shown in Fig.(17). It demonstrates that the total amount of water infiltrated along the whole valley length is estimated to be 38.51 million  $m^3$ , which is equivalent to 71.8% of the total inflow. Fourteen percent of this amount infiltrated through the part of the valley south to Nakl city, where as sixteen percent infiltrated through the last 28 Kilometers.

The amount of inflow, amount of losses and the amount of outflow at different sections along the valley are shown in Fig.(18), it indicates that the total surface runoff lost into the Mediterranean Sea is about 14 millions  $m^3$  which is equivalent to 26.74% of the total inflow. The maximum value of water outflow occurred at Kilometrage 196. This is a significant factor in the choice of a convenient location for building a dam. Other factors of equal importance are sedimentary formation in this site has a minimal rate of infiltration, the topographic configuration at location supports its choice at this site; the channel was found significantly narrow surrounded by two high mountains and preceded by significantly wide part of the channel, therefore this location is considered a convenient location for installing a dam.



CONCLUSIONS  
-----

The present study demonstrated essential data for predicting the most convenient location for a dam to restore considerable amount of runoff, since the water lost in the Mediterranean Sea is too significant not to be neglected. Attention should be directed towards allocation of several scattered single dams and a series of small dams all over the valley in addition to a great number of ponds carefully selected in order to save an optimum amount of restored fresh water.

More than seventy percent of the surface runoff could take its course through infiltration passages and reaches ground water reservoir. Fortunately the maximum quantity of infiltration occurs at El-Arish zone. This will diminish the loss in the Mediterranean Sea by balancing out consumptive uses against the stored water reservoir and that replenish and feed the aquifer. Further studies should be directed towards investigations concerning the interrelationship parameters and cross correlations of ground water against surface runoff. Researches are recommended towards a proposed mathematical model describing such relationship in balancing manner.

One of the very useful information of the present study offered is determining the lag time which is important to predict the time onset of maximum discharge and the highest water levels to be expected, so the people in this area can be warned before hand, avoiding higher water level effects and minimizing any resulting damages.

Water mangement studies, based on more accurate meteorological data, are highly recommended for this area as the water resources are considerably scarce and limited.

## APPENDIX (I): REFERENCES

- 
1. Chen, C.L., "An Analysis of Overland Flow", Ph.D. Dissertation, Michigan State University, East Lansing, 1962.
  2. Chen, C.L. and Hansen V.E., "The Theory and Characteristics of Overland Flow", Presented at the Winter Meeting of the American Society of Agricultural Engineers, Chicago, Illionis, 1963.
  3. Chow, V.T., "Open Channel Hydraulics", McGraw Hill Book Company, New York, 1959.
  4. El-Gamal, M. "Hydraulics of Overland Flow", Ph.D. Thesis, Water Engrg. Dept., Zagazig Univ., 1984.
  5. El-Ramli, M.E., "Studies of Torrents in Wadi El-Arish Basin", General Development Authority, Cairo, Egypt, 1965 (in Arabic).
  6. El-Shazly, E., Abdul Hadi, M., Ghawaby, M. , El-Kassas, T. and El-Shazly, M.", "Geology of Sinai Peninsula from ERTS-1 Satellite Image", the Remote Sensing Project, Academy of Scientific Research and Technology, Cairo, Egypt, 1973.
  7. Graf, W.H., "Hydraulics of Sediment Transport", McGraw Hill Book Company, New York, 1971.
  8. Holtan, H.N. "A Concept for Infiltration Estimates in Watershed Engineering", U.S. Department of Agriculture, Agricultural Research Service, 1961.
  9. Kijne, J.W., "Surface Irrigation", Irrigation Dept., University of Nairobi, Nairobi, 1977.
  10. Linsley, R.K., Kohlar, M.A. and Paulhus, J.L. "Hydrology for Engineers", McGraw Hill Book Company, New York, 1975.
  11. Varshney, R.S., "Engineering Hydrology", 2nd Ed., Nem Chand & Bros, Roorkee, India, 1978.
  12. Zidan, A.R., "A Hydraulic Investigation of the River Forth", Ph.D. Thesis, University of Strathclyde, Scotland, 1978.

APPENDIX (II): NOTATION

The following symbols are used in this paper:

$A_b$	= area of the watershed of the tributary;
$a_b$	= empirical constant of the infiltration rate;
$B$	= top width of flow;
$B_s$	= bed slope effect;
$b$	= empirical exponential constant of the infiltration rate;
$b_1$	= empirical exponential constant of the lag time;
$C^+$	= forward characteristics;
$C^-$	= backward characteristics;
$c_p$	= coefficient for maximum discharge per square kilometre;
$c_t$	= lag time coefficient;
$D$	= hydraulic depth;
$D_A$	= change in geometry effect;
$D_t$	= average duration time of the storm;
$d_{50}$	= diameter through which fifty percent; of the sample can pass;
$E$	= evaporation rate;
$E_I$	= evaporation effect;
$F_S$	= friction effect;
$g$	= gravitational acceleration;
$K_I$	= runoff coefficient;
$L_c$	= distance from the outlet to the centroid of the watershed;
$L_1$	= length of the main channel;
$N_I$	= infiltration effect;
$n$	= Manning's roughness coefficient for the valley;
$n_o$	= Manning's roughness coefficient for straight uniform and smooth channel;
$Q_p$	= peak discharge in cumecs;
$Q_L$	= lateral inflow from the tributary;
$q$	= lateral inflow per unit length;
$q_I$	= lateral inflow effect;
$q_p$	= maximum discharge per square kilometre;
$R$	= average intensity of rainfall due to the storm;
$R_I$	= rainfall effect;
$r$	= rainfall rate;
$S$	= basin slope;
$S_f$	= friction slope;
$S_o$	= channel bed slope;
$T$	= time base of hydrograph;
$t$	= time;
$t_p$	= lag time in hours;
$u$	= velocity of flow;
$W_{75}$	= width of synthetic hydrograph at ordinate 75% of the peak discharge;
$W_{50}$	= width of synthetic hydrograph at ordinate 50% of the peak discharge;
$x$	= distance measured along the flow direction;
$y$	= depth of flow;
$\delta t$	= time increment,
$\delta x$	= space increment; and
$\beta$	= momentum coefficient.